Proceedings of the IASS 2024 Symposium
Redefining the Art of Structural Design
August 26-30, 2024, Zurich Switzerland
Philippe Block, Giulia Boller, Catherine DeWolf,
Jacqueline Pauli, Walter Kaufmann (eds.)

The effect of geometric tiling parameters on the stiffness of a rotational kirigami system

Isabel M. DE OLIVEIRA [a,*], Emily BAKER[b], Sigrid ADRIAENSSENS[a]

[a] Princeton University
59 Olden St. (CEE) E209A, Princeton, NJ
* imdo@princeton.edu

[b] University of Arkansas

Abstract

Sheet metal structures are widely used in the construction industry and have applications in building façades, roof structures, and bridge cladding. To address the relatively low bending stiffness of sheet metal, most of these structures require individually added stiffeners fabricated from multiple sheets. We leverage kirigami principles to eliminate the number of discretely added parts and increase fabrication efficiency. In particular, we study a rotational triangular kirigami system that forms a plate-lattice space frame system once each unit cell is deployed and connected to adjacent cells. This frame exhibits enhanced load-carrying capacity and stiffness. The present work focuses on understanding how variations in geometric parameters of a triangular tiling of one unit affect the stiffness of the rotational kirigami space frame. By generating a linear elastic finite element model using beam elements, we use the frame's elastic energy for a comparative performance analysis between the different models. We show that, while maintaining the same size and position of the connected hubs, the larger the rotation of the base triangles, the higher the maximum displacement. Tabletop experiments validate the results qualitatively. An automated parametric model enables design space exploration. Understanding how geometric parameters control the stiffness of the space frame enables the design and creation of deployable and stiff kirigami-based space frames suitable as large-scale structural building components.

Keywords: kirigami, space frame, finite element model, parametric design.

1. Introduction

Sheet metal structures are widely used in the construction industry and have applications in building façades and roof structures, bridge cladding, and industrial catwalks [1], [2]. To overcome their low bending stiffness, most sheet metal structural components require individually added stiffeners fabricated from multiple sheets or external supporting structures [3], [4]. We leverage origami/kirigami principles to eliminate the number of discretely added parts and increase fabrication efficiency [5], [6], [7]. In particular, we study a rotational kirigami system known as spin-valence that forms a plate-lattice space frame once each unit cell is deployed and connected to adjacent cells [6], [8]. This frame exhibits enhanced load-carrying capacity and stiffness under out-of-plane compression [9], [10], [11], showing promise for load-carrying applications.

While the structural capacity of the system of a single tiling pattern has been previously studied [9], [10], the effects of variations of the pattern on the structural behavior are lacking. To study pattern variations, we use simplified modeling assumptions to compare structural responses among the different system configurations. The simplified modeling assumptions are expected to underpredict the structure's displacements, but these comparative analyses can be useful to build a more fundamental understanding of the system and aid future design decisions. Simplifications include assumptions such as: (1) the

system components deploy as infinitely rigid bars rotating about zero-stiffness rotational hinges (i.e., linkages); (2) geometric complexity of the 2D cut pattern can be captured by a 1D line-element structure; and (3) constant cross-sections.

Using the deployment definition available from the literature [12], [13] to find the deployed shape, we vary one geometric parameter and generate different system configurations for analysis and comparison. Thus, the present work aims to understand how variations in the pattern geometry affect the stiffness of a triangular tiling rotational kirigami space frame under compressive out-of-plane loading and to qualitatively validate these assumptions with tabletop experiments. It is hypothesized that models with smaller eccentricities and higher structural depth generate stiffer space frames.

2. Materials and methods

To study the variations in geometric parameters of the space frame system, we first generate a parametric model of line segments representing the main system components (see Section 2.1): base polygon, primary and secondary legs, and the hub (see Figure 1). These lines, positioned at the centroidal axis of the elements, are then used as the basis to generate two models: the finite element (FE) model of the deployed configurations (see Section 2.2) and the cut pattern for fabrication and experimentation (see Section 2.3).

2.1. Geometry

The system is comprised of (1) a base polygon which defines the external boundary of each unit cell component (see the blue triangles of Figure 1); (2) hubs which are polygons nested inside the base polygon geometry (see red triangles in Figure 1); and (3) primary legs which connect vertices of the base polygon and the hub (see gray lines in Figure 1). Figure 1(a) to (b) shows how the hub deploys according to the parallel deployment definition from the literature [12], [13]. This deployment definition is described by the intersection of the sphere centered at the leg endpoint lying on the base polygon and the cylinder circumscribed about the hub polygon.

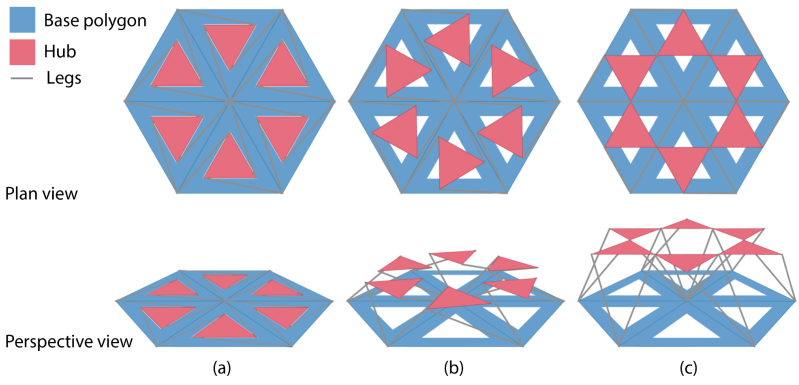

Figure 1: The system comprises a base polygon, legs, and a hub: the (a) initially flat hub (b) rotates as it deploys out of the plane until it reaches a (c) final position connecting all system components in a triangulated manner.

The software used for geometric modeling is Rhino3D/Grasshopper [14]. The model is generated first by creating a regular triangular grid with the dimensions specified in Table 1. To enable control of the primary surface boundary polygon configurations, the depth of the space frame system is allowed to change with the rotation of the base polygons. The depth *d* is indicated in Figure 2 for each configuration.

Table 1: System dimensions for the four space frame configurations.

Model specification	Dimension (m)
x-direction span	4
y-direction span	3
z-direction deployed depth *d* for (0º; 10º; 20º; 30º) configurations	(0.16; 0.19; 0.21; 0.23)
Unit diameter	0.4
Cross-section widths of (hub; leg; base polygon) elements	(80; 40; 100) * 10^{-3}
Material thickness	3.03 * 10^{-3} (gauge 11)

Figure 2 shows the four geometric configurations used in this study. First, the base polygons are aligned with the triangular grid pattern, generating the 0º rotation configuration. Then, the base polygons are rotated by different angles θ with respect to the grid to generate the other three configurations. The base polygons are concurrently scaled by *cos (θ)* to maintain the connection of adjacent cell edges. We note that the central region of a collection of six adjacent triangles connects at a single point in the 0º rotation configuration (see 0º rotation in Figure 2). However, as the rotation increases, the edges no longer connect at a single point. This factor is expected to increase the eccentricity of the flow of forces at the structural analysis stage, and thus, this quantity is highlighted with the variable $e_{rotation}$ in the 30º rotation in Figure 2. The four configurations maintain hubs with fixed geometry and fixed point-to-point connectivity between adjacent unit cells.

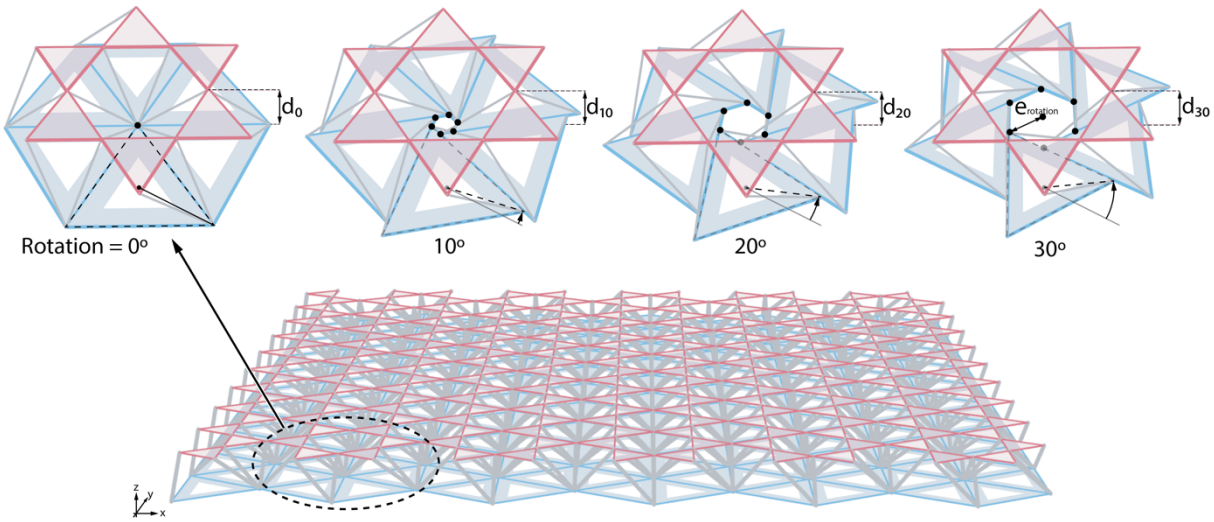

Figure 2: A geometric model of four space frame configurations with varying base polygon rotations (in blue). Hubs' (in red) geometry and positions remain the same for all configurations, but the depth of the space frame changes according to the deployment definition. (See Table 1 for dimensions.)

2.2. Finite element model

Karamba3D [15] is used for FE modeling under the assumptions of small displacements in the linear elastic regime. The FE analyses are conducted on the already deployed space frame from Section 2.1. Each system component is modeled using six degrees of freedom beam elements with fixed thickness and constant cross-sectional width along the beam's longitudinal axis (see Table 1 for dimensions). The constant widths simplify the cut pattern shown in Section 2.3 to reduce model complexity. Additionally, all nodal connections of the patterns are modeled with full nodal continuity (bending moments are

transferred) and assumed to have no additional eccentricity due to the differences in actual fabricated geometry (see $e_{fabrication}$ *in* Figure 3). The only eccentricities present in the FE model correspond to the change in global geometry due to applied rotations at the base polygons highlighted with the variable $e_{rotation}$ in Figure 2. The 0º rotation configuration in particular is assumed to have no eccentricity of any kind in the FE model.

The material used for analyses is steel with a modulus of elasticity of 210 GPa and Poisson's ratio of 0.3. The edges along the y-direction have pinned support conditions on the left side and roller support conditions on the right side. A load of $1.5kN/m^2$ is uniformly applied to the top nodes of the structure and gravity loads are not applied. A first-order analysis component is used, and the total elastic energy is recorded alongside the maximum nodal displacement of the system for each configuration. The boundary conditions can be visualized in Figure 4 of Section 3.1.

2.3. Experiments

Tabletop experiments were carried out by laser cutting 4-ply Bristol paper to produce 0º and 30º pattern rotations, each of which measured 180mm x 360mm in plan. Once deployed, neighboring units were glued at their connections producing stiff space frames. Each model was placed on two supports at the short ends, producing a span. A piece of paper was placed on top of each model, and distributed loading was simulated by placing small cans of consistent weight (85g) at approximately 70mm on center in a grid of nine cans on top of the models. Images were taken at each stage of loading and the two models were compared. Figure 3 shows section of the fabricated models with the cut pattern overlaid on the line model described in Section 2.1. This figure also highlights the two types of eccentricities and shows the original triangular pattern used as a base for all geometries in dashed lines.

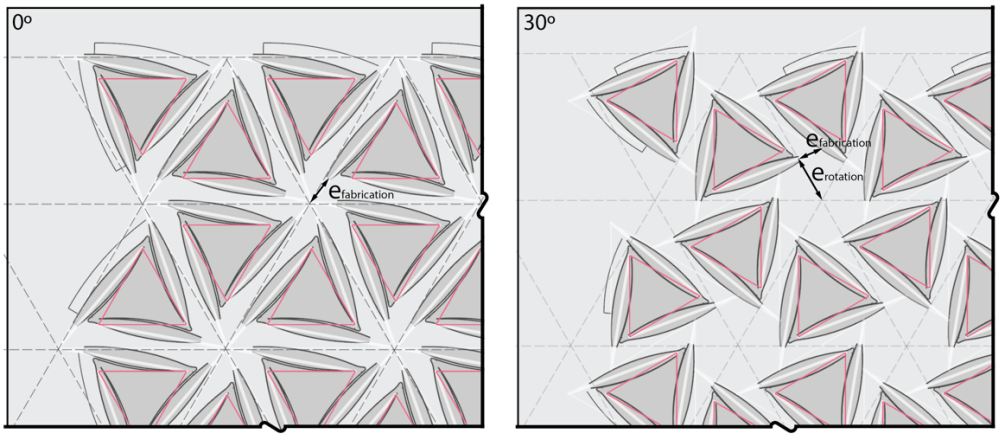

Figure 3: A section of the cut pattern for the 0º rotation model shows the eccentricity present in the fabrication but neglected in the FE models ($e_{fabriaction}$). The 30º rotation model section shows $e_{fabriaction}$ and the eccentricity generated by rotating the base polygons ($e_{rotation}$) which is accounted for in the FE models.

3. Results and discussion

This section includes results showing that, while maintaining the same size and position of the connected hubs, the more the base triangles rotate, the less stiff the frame is (see Section 3.1). Section 3.2 shows how tabletop experiments qualitatively validate the numerical results. Section 3.3 studies the effect of the change in a space frame depth on its maximum displacements compared to the spin-valence space frame.

3.1. Finite element model results

Figure 4 shows simply supported boundary conditions imposed along the y-direction edges for the FE analyses. The figure shows the displacement response in the perspective view with a blue-to-red color gradient. Higher displacement values are shown in red nearer the middle of the span, as shown in the elevation view in Figure 4.

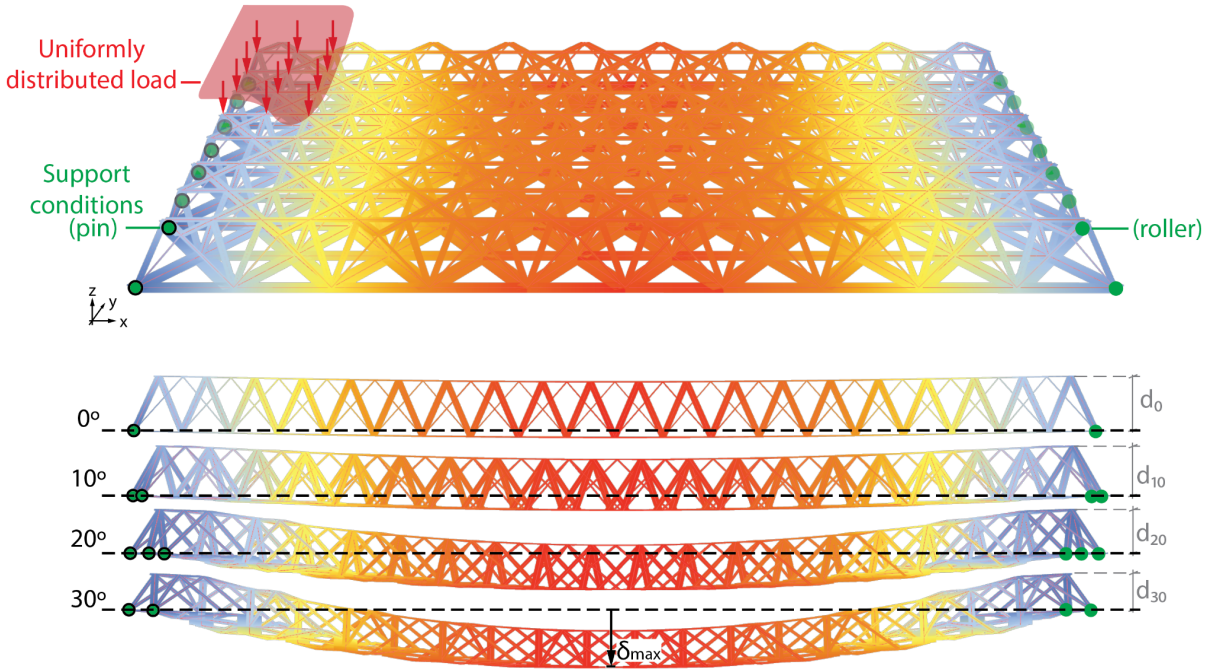

Figure 4: Displacements of a single span simply supported space frame due to a uniformly distributed load applied at the top nodes. Deformations scaled by 20 times are shown for the four configurations.

For higher base polygon rotation values, there is an associated increase in maximum displacements and, similarly, in the system's total elastic energy, as shown in Table 2. There are two explanations for this increase in displacements related to the global geometry of the structure: (1) there is an increase in rotation eccentricities ($e_{rotation}$), and (2) there is a decrease in the structural depth of the space frame (d). However, it must be noted that these results neglect buckling effects, and there could be changes in these results due to changes in the legs slenderness ratios between different configurations. Future work will include such analyses.

Table 2: Results from the FE analysis for each space frame configuration.

Rotation angle (deg)	δ_{max} (mm)	Energy (kN.m)
0	1.38	0.00504
10	3.04	0.01115
20	7.53	0.02690
30	11.50	0.04295

The unit rotation and out-of-plane displacements are coupled, therefore, making it more challenging to analyze the sensitivity of each modeling parameter. The change in depth of a regular space frame system was conducted in Section 3.3 as a reference. Furthermore, the higher the eccentricity is between base polygons, the more material is left uncut from the fabricated modules in the eccentricity region. This factor could aid in reducing the displacements observed in the experimental models compared to the FE models which currently account for voided regions in the areas between adjacent triangular units.

3.2. Experiments

Figure 5 shows results from tabletop experiments for a qualitative validation of numerical simulations. The results show that the 0º rotation model deflects less than the 30º rotation model, agreeing with the results presented in Section 3.1.

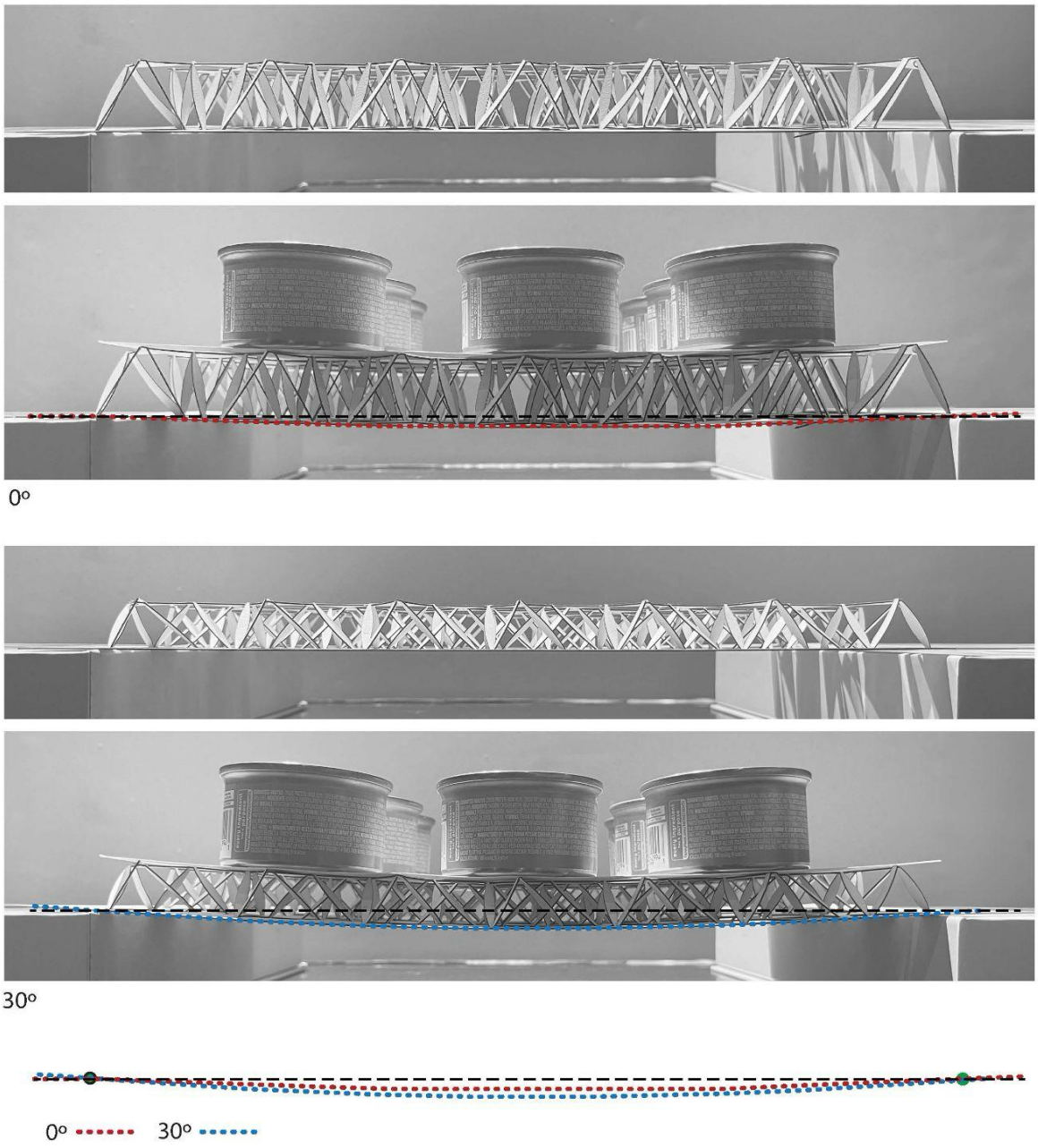

Figure 5: Displacements of 0° and 30° space frame models made of laser cut paper with uniformly distributed loading.

3.3. The effect of change in depth in the space frame's displacements

The spin valence space frame presents higher displacements due to both increase in eccentricities caused by base polygons rotations and reduction of the system's structural depth. Both factors are coupled in that system. We analyze space frames of the 0º rotation configuration scaled in the z-direction to understand how the system would behave if it did not have coupled depth and base rotations. While all other dimensions of the FE model remain constant for the 0º rotation configuration, the z-direction is scaled to match the depths provided in Table 1.

Figure 5 shows that there is a decrease in displacements with a higher-depth structural system. However, this comparison shows that the change in displacements of the spin-valence space frame is not explained by that factor alone. The added eccentricities of nodal connections on the more rotated configurations contribute significantly to the deformations of the spin-valence space frame. The eccentricity ($e_{rotation}$) contribution is particularly significant for the models with 20º and 30º rotations. The preliminary analyses of the present work show that the maximum displacements of the spin valence system are below or equal to the allowable serviceability deflection limit of *1/360* of the span under live loads [16], which correspond to *11 mm*. While this result shows promise for floor system applications, it is noteworthy that the FE model neglects uncut material from the rotated configurations in the eccentricity area, and it also assumes the system remains in the linear elastic regime without buckling. Further studies should consider these factors to provide more realistic deflection estimations. Nevertheless, the current models indicate they can indeed be used for early-stage design exploration of the system.

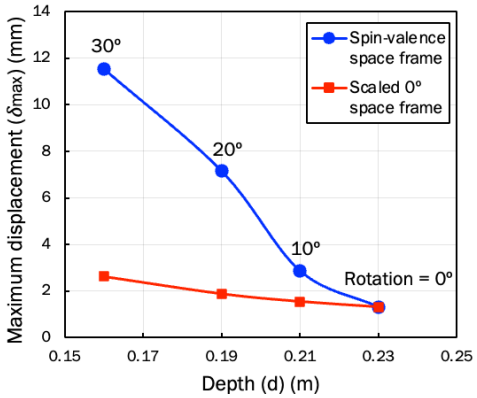

Figure 6: Comparison of the change in maximum displacement due to the change in structural system depth. The 0º rotation space frame was scaled in the z-direction while all other dimensions and FE modeling parameters remained the same.

4. Conclusion

From the study presented herein, we conclude that increasing the system's depth and decreasing base polygon connection eccentricities reduces the system's maximum displacements under simply supported and uniformly distributed load conditions. These characteristics are associated with configurations with smaller base polygon rotation and confirm the initial hypothesis stated in Section 1. From the qualitative assessment of the numerical models compared with tabletop experiments, we observed that the FE modeling assumptions satisfactorily predict which configuration deflects more than the other. Therefore, we can use simplified modeling assumptions to generate comparative studies like the one presented herein. These models remain unsuitable for direct structural response predictions such as actual system stresses and deformations. To that end, eccentricities, variations in cross-sectional widths, and buckling must be considered, as developed in related work [11]. Ultimately, understanding how triangular tiling geometric parameters control the structural stiffness of the space frame enables the design and creation of deployable and stiff kirigami-based space frames suitable as large-scale structural building components.

Acknowledgements

The first and last authors acknowledge funding provided by the NSF Institute for Data-Driven Dynamical Design (ID4), OAC #2118201.

References

[1] D. Smith, C. Graciano, and G. Martínez, "Expanded metal: A review of manufacturing, applications and structural performance," *Thin-Walled Structures*, vol. 160, p. 107371, Mar. 2021, doi: 10.1016/j.tws.2020.107371.

[2] J. M. Rico-Martinez, M. Brzezicki, C. G. Ruiz-Mugica, and J. Lech, "Daylight transmittance through expanded metal shadings," *Journal of Facade Design and Engineering*, pp. 85-114 Pages, Nov. 2020, doi: 10.7480/JFDE.2020.1.4698.

[3] T. Helbig, L. Giampellegrini, and M. Oppe, "'Carioca Wave' – A free-form steel-and-glass canopy in Rio de Janeiro, Brazil," *Steel Construction*, vol. 7, no. 4, pp. 252–257, Nov. 2014, doi: 10.1002/stco.201420033.

[4] "Chrysalis Amphitheater," Mark Fornes / Theverymany. Accessed: Apr. 15, 2024. [Online]. Available: https://theverymany.com/buildings/13_merriweather-park

[5] S. E. Calisch and N. A. Gershenfeld, "Towards continuous production of shaped honeycombs," in *Volume 3: Manufacturing Equipment and Systems*, College Station, Texas, USA: American Society of Mechanical Engineers, Jun. 2018, p. V003T02A007. doi: 10.1115/MSEC2018-6646.

[6] E. Baker, "Search for a rooted aesthetic: study in spin-valence," in *Fabricate 2014: Negotiating Design & Making*, UCL Press, 2014, pp. 128–135. doi: 10.2307/j.ctt1tp3c5w.

[7] Y. Miyamoto, "Rotational erection system (RES): Origami extended with cuts," in *Origami*, Providence, Rhode Island: American Mathematical Society, 2015, pp. 537–544. doi: 10.1090/mbk/095.2/16.

[8] M. Ramirez, E. Baker, E. Harriss, and G. Herning, "Double-curved spin-valence: Geometric and computational basis," in *AAG 2020*, Paris, 2020, pp. 408–425. [Online]. Available: https://thinkshell.fr/advances-in-architectural-geometry-2020-on-line-library/

[9] N. Sherrow-Groves and E. Baker, "Structural finite-element analysis of steel kirigami space frame to characterize global behavior," in *Form and Force*, Barcelona: International Association for Shell and Spatial Structures, 2019, pp. 1757–1764.

[10] J. Sahuc, G. M. Herning, and E. Baker, "Experimental and analytical investigation of the spin-valence kirigami space frame," in *Form and Force*, Barcelona: International Centre for Numerical Methods in Engineering (CIMNE), 2019, pp. 1733–1740.

[11] I. M. de Oliveira, E. M. Sosa, E. Baker, and S. Adriaenssens, "Experimental and numerical investigation of a rotational kirigami system," *Thin-Walled Structures*, vol. 192, p. 111123, Nov. 2023, doi: 10.1016/j.tws.2023.111123.

[12] M. Ramirez, E. Baker, E. Harriss, and G. Herning, "21: Double-curved spin-valence geometric and computational basis - Baker et al," 2021. Accessed: Dec. 06, 2021. [Online]. Available: https://www.youtube.com/watch?v=UxQYpxoTeZ0&t=153s

[13] E.-M. Graefe, H. J. Korsch, and M. P. Strzys, "Bose–Hubbard dimers, Viviani's windows and pendulum dynamics," *J. Phys. A: Math. Theor.*, vol. 47, no. 8, p. 085304, Feb. 2014, doi: 10.1088/1751-8113/47/8/085304.

[14] "Rhino3D®." Robert McNeel & Associates. [Online]. Available: www.rhino3d.com

[15] C. Preisinger, "Linking structure and parametric geometry," *Archit Design*, vol. 83, no. 2, pp. 110–113, Mar. 2013, doi: 10.1002/ad.1564.

[16] American Institute of Steel Construction, *Specification for structural steel buildings: Allowable stress design and plastic design*. Chicago: American Institute of Steel Construction, 1989.